Cellular Physiology and Biochemistry

Cell Physiol Biochem 2020;54:303-320
DOI: 10.33594/000000221
Published online: 8 April 2020
Accepted: 22 March 2020

Original Paper

Preferential Killing of Tetraploid Colon Cancer Cells by Targeting the Mitotic Kinase PLK1

Mohamed Jemaà[a] Chamseddine Kifagi[b] Sonia Simon Serrano[a] Ramin Massoumi[a]

[a]Department of Laboratory Medicine, Translational Cancer Research, Faculty of Medicine, Lund University, Lund, Sweden, [b]Division of Immunology and Vaccinology, Technical University of Denmark, Copenhagen, Denmark

Key Words
Colon Cancer • Tetraploidy • PLK1 • Mitosis • Apoptosis • Synergy • Microtubules agents

Abstract
Background/Aims: Chromosomal instability is a well-known factor in the progression of different types of cancer, including colorectal cancer. Chromosomal instability results in severely rearranged karyotypes and aneuploidy. Tetraploidy constitutes an intermediate phase during the polyploidy/aneuploidy cascade in oncogenesis, and tetraploid cells are particularly resistant to chemotherapy. Whether inhibition of the mitotic protein polo-like kinase 1 (PLK1) prevents the survival of tetraploid colon cancer cells is unknown. ***Methods:*** Diploid and tetraploid cells were transfected with siPLK1 or treated with PLK1 inhibitor Bi2536 in combination with spindle poison. Cell toxicity was assessed via crystal violet staining and clonogenic assay. Flow cytometry assessment analyzed numerous cell apoptotic parameters and cell cycle phases. Synergistic activity between Bi2536 and paclitaxel, vincristine or colchicine was calculated using the CompuSyn software. ***Results:*** Inhibition or abrogation of PLK1 prevented the survival of colon cancer cells, specifically tetraploid cells. The cell death induced by PLK inhibition was due to mitotic slippage, followed by the activation of the intrinsic pathway of apoptosis. We further demonstrated that co-treatment of the tetraploid colon cancer cells with a PLK1 inhibitor and the microtubule polymerisation inhibitor vincristine or colchicine, but not the microtubule depolymerisation inhibitor paclitaxel, provoked a lethal synergistic effect. ***Conclusion:*** PLK1 inhibition together with microtubule-targeting chemicals, serve as a potent therapeutic strategy for targeting tetraploid cancer cells.

M. Jemaà and R. Massoumi share senior co-authorship.

Dr. Mohamed Jemaà
and Dr. Ramin Massoumi

Department of Laboratory Medicine, Translational Cancer Research,
Lund University, Lund 22381 (Sweden)
Tel. +46 46 222 64 30, E-Mail mohamed.jemaa@med.lu.se, ramin.massoumi@med.lu.se

Introduction

Colorectal cancer (CRC) is one of the most commonly diagnosed cancers and a leading cause of death worldwide. CRC represents 10% of all diagnosed tumours in men and 9.2% in women, and its global incidence is estimated at 1.4 million cases annually, with 700,000 deaths in 2012. Moreover, the CRC incidence is expected to increase 60% by 2030, to more than 2.2 million new cases and 1.1 million cancer deaths [1, 2]. Identifying an efficient treatment is thus crucial to reduce the CRC morbidity rates. One of the cancer hallmarks in general, and CRC in particular, is genomic instability. This phenomenon increases the probability of oncogenic events and creates a heterogeneous cell population with extensive abilities to adapt and evolve [3]. Tetraploidy is a state that can lead to aneuploidy and genomic instability [4-6]. Tetraploidy represents the condition of having twice as many chromosomes compared to their normal, diploid counterparts [7, 8]. Tetraploidy can arise from endoreplication (DNA replication without mitosis) [9], endomitosis (karyokinesis without cytokinesis) [10, 11] or aberrant cell fusion [12]. Tetraploid cells are frequently found in pre-neoplastic lesions of intestinal cancers [13-15].

The persistence of a tetraploid population is often correlated with the inactivation of tumour suppressors retinoblastoma 1 (RB1) and tumour protein p53 [5]. Inactivation of p53 facilitates the tetraploidisation of cell lines [16, 17]. Similarly, mutations that inactivate the adenomatous polyposis coli (APC) tumour suppressor gene initiate a majority of colorectal cancers and result in tetraploidisation *in vitro* and *in vivo* [18]. Tetraploid cells are intrinsically resistant to genotoxic stress mediated by ionising irradiation or anti-cancer chemotherapeutic agents, including platinum compounds and topoisomerase inhibitors [19, 20]. Thus, tetraploid cells might contribute to chemotherapeutic failure. The development of novel strategies to target tetraploid tumour cells can improve the treatment outcome for CRC patients.

PLK1 is a member of the polo-like kinase (PLK) family and mediates several key functions throughout mitosis, including bipolar arrangement of the centrosomes, the spindle assembly checkpoint and cytokinesis [21-23]. PLK1 is located in different subcellular compartments depending on its function. PLK1 is mostly cytoplasmic during the interphase. During early mitosis, PLK1 is accumulated at the spindle poles, then in the kinetochores for chromosomal alignment in the metaphase plate and concentrated in the cytokinetic bridge during cytokinesis [24, 25]. PLK1 expression levels are elevated in a range of different tumor types, including invasive breast carcinoma, hepatocellular carcinoma and CRC [26]. PLK1 can promote tumorigenesis in a myriad of ways. First, PLK1 can phosphorylate MDM2 or p53 and abrogate the p53 function. Second, PLK1 can increase the levels of the oncogenic transcription factor MYC in a positive feedback loop. Third, PLK1 overexpression leads to degradation of the tumour suppressor repressor element-1 (RE-1) silencing transcription (REST) in triple negative breast cancer. Fourth, mainly in hepatocellular carcinoma, hepatitis B can stimulate PLK1 activation, an action that leads to the repression of several transcription factors, including SUZ12 and ZNF198. Finally, PLK1 can also inhibit the tumour suppressor phosphatase and tensin homolog (PTEN) and thus indirectly activate the oncogenic phosphoinositide 3-kinase (PI3K) pathway [27].

Here, we report that PLK1 inhibition leads to the selective destruction of tetraploid cancer cells. In addition, we provide a complete characterisation of the pro-apoptotic signal transduction pathway provoked by PLK1 inhibition and the benefit of using a combination treatment with anti-microtubule polymerisation agents.

Materials and Methods

Cell lines, culture conditions and reagents

Diploid and tetraploid clones derived from human colon carcinoma RKO and HCT116 cells were routinely maintained in McCoy's 5A medium supplemented with 10% fetal calf serum (FCS), 10mM HEPES buffer, 100units/mL penicillin G sodium and 100µg/mL streptomycin sulfate (all provided from Thermo Fisher Scientific-Gibco, Waltham, MA). Diploid and tetraploid clones derived from MFH152 sarcoma cells line were grown in Dulbecco's modified Eagle's medium (DMEM) supplemented with 10% FCS and antibiotics. Both RKO and HCT116 clones are p53 WT, while MFH152 clones are p53 mutated. Cells were routinely maintained at 37°C under 5% CO_2.

Chemicals

Bi2536 (Sigma-Aldrich) was stocked at 20 mM. Pifithrin-α (Sigma-Aldrich) was stocked at 20 mg/ml. The pan-caspase inhibitor z-VAD-fmk (Sigma-Aldrich, Germany) was stocked at 50 mM. The necroptosis inhibitor Necrostatine-1 (Sigma-Aldrich, Germany) was stocked at 100 mM. The appropriate amount of DMSO was always employed for negative control conditions.

Clonogenic survival assay

Cells were seeded at low concentrations (1000 cells/well of 6-well plate) and were left untreated or treated with increasing doses of the PLK1 inhibitor Bi2536. 2 assays were performed. First using a continuous treatment for 2 weeks, or with a washout at 24h followed by culture in standard conditions for up to 15 days. Colonies were then fixed/stained with aqueous crystal violet and counted.

For each treatment, the surviving fraction (SF) was estimated according to the formula: SF = (number of colonies formed in control condition/number of colonies formed in treatment condition).

RNA interference

Cells were seeded at low density in 6-well plates and after 24 h transfected with a non-targeting siRNA (siUNR) with a sequence unrelated to the human genome (UNR, sense 5'-GCCGGUAUGCCGGUUAAGUdTdT-3'), with siRNAs directed against PLK1 mRNA (siPLK1a, ON-TARGETplus SMARTpool, L-003290–00-0005; GE Dharmacon, Lafayette, CO, siPLK1b, #ID AM51331 and siPLK1c, ID AM16708, Thermo Fisher Scientific) by means of oligofectamine RNAiMAX transfection reagent (Thermo Fisher Scientific-Invitrogen), according to the manufacturer's instructions. Transfection efficiency was determined by western blot and real time PCR.

Quantitative PCR

The cells were rinsed in cold PBS and total RNA extracted using RNeasy Mini kit (Qiagen, #74106) and performed according to manufacturer's instruction. The purity of RNA was analyzed and quantified by a NanoDrop 2000 spectrophotometer (Thermo Fisher) and used for cDNA synthesis according to the manufacturer's instruction (High Capacity cDNA Reverse transcription kit #4368814, Applied Biosystems). PCR runs were performed in the QuantStudioTM 7 Flex System using SYBR®Green Reagent (Applied Biosystems), with the following program; 2 min 50 °C, 10 min in 95 °C followed by 40 three-step cycles consisting of 95 °C for 20 s and 60 °C for 30 s and 72 °C for 1 min. The PLK1 relative expression was quantified using the following primers: Forward primer: TCAAGGAACCTCTGGTGTCA and Reverse primer: GGTTACTCTCTGGAACCTCTGGT. GAPDH (Forward primer: TGCACCACCAACTGCTTAGC and Reverse primer: GGCATGGACTGTGGTCATGAG) and actin (Forward primer: AGAGCTACGAGCTGCCTGAC and Reverse primer: AGTACTTGCGCTCAGGAGGA) were used as housekeeping genes.

Western blotting

Cells were lysed in 8M urea denaturing lysis buffer (8M Urea, 100 mM Na2HPO4, 100 mM NaH2PO4, 10 mM Tris/HCl pH 8 and 5 mM DTT). 15 µg of each sample was subjected to PLK1 western blotting (Thermo Fisher Scientific, # # 33-1700) using HRP-conjugated goat anti-mousse as a secondary antibody (Life Technologies, A16054). After ECL development the blot was re-probed with anti α-tubulin (Sigma-Aldrich, SAB4500087) followed by rabbit anti-mouse-HRP (abcam, #ab6728).

Cristal Violet proliferation assay

Cells were seeded in 96-well plates with a 5000-cells/well density. 24 hours later, cells were treated or not with Bi2536 or DMSO, or transfected with siUNR or siPLK1 for up to 3 days. Cells were fixed with 4% paraformaldehyde (PFA) for 30 min. Then after, PFA was removed and cells were stained for 30 min at room temperature with aqueous solution containing 0.1% (w/v) crystal violet. Cells were washed three times with distilled water before the administration of 200 µl/well of 10% acetic acid and shaking with micropipettes. The absorbance of each sample was measured using a scanning microplate spectrophotometer (Synergy 2, Biotek, Germany) reader by absorbance detection at 595 nm.

Cytofluorometric studies

Cytofluorometric acquisitions were performed by means of a FACSVerse cytofluorometer (BD Biosciences). Data were statistically evaluated using the FCS Express 6 Flow (De Novo Software, CA, USA) software.

1/ Cell cycle analysis and subG$_1$ quantification. For the quantification of cells cycle profiling (DNA content), cells were fixed with 75% (v/v) ethanol in PBS, DNA was stained with propidium iodide and analyzed with the cytometer. To quantity the apoptotic and DNA fragmented fraction we measured the subG$_1$ population in the cell cycle. The PI is measured with an excitation wavelength of 488 nm (blue laser) and an emission wavelength of 695 nm on the PerCP-Cy5.5 channel.

2/ Measurement of cell permeabilization. For the quantification of plasma membrane integrity, cells were harvested and collected with the culture medium and stained with 0.5 to 1 µg/mL Propidium Iodide (PI), which only incorporates into dead cells, from ThermoFisher) for 30 min at 37°C before FACS assessment. The PI is measured with an excitation wavelength of 488 nm (blue laser) and an emission wavelength of 695 nm on the PerCP-Cy5.5 channel.

3/ Measurement of mitochondrial membrane potential. For the simultaneous quantification of plasma membrane integrity and mitochondrial transmembrane potential (Δψm), cells were harvested and collected with the culture medium and stained with 1 µg/mL propidium iodide and 40 nM 3, 3'-dihexyloxacarbocyanine iodide (DiOC$_6$(3), a Δψm-sensitive dye) (Molecular Probes-Invitrogen, Eugene, OR, USA) for 30 min at 37 °C before FACS assessment. The DiOC$_6$(3) is measured with an excitation wavelength of 488 nm (blue laser) and an emission wavelength of 530 nm.

4/ Measurement of cell scrambling and phosphatidylserine exposure. For the quantification of phosphatidylserine exposure, cells were harvested and collected with the culture medium and stained with Annexin-V-FITC (1:200 dilutions; ImmunoTools, Friesoythe, Germany) for 30 min at 37 °C before FACS assessment. The FITC is measured with an excitation wavelength of 488 nm (blue laser) and an emission wavelength of 530 nm.

5/ Measurement of intracellular Calcium concentration. For the evaluation of the cytosolic Ca^{2+}, cells were collected and suspended in growth medium loaded with 5 µ M of the calcium tracker Fluo-3/AM (Biotium, Hayward, CA, USA). The cells were incubated at 37 °C for 30 min before Ca2+-dependent fluorescence intensity measurement. The Fluo-3 AM is measured with an excitation wavelength of 488 nm (blue laser) and an emission wavelength of 530 nm. The signal shift was measured comparatively to non-treated cells.

6/ Measurement of caspase 3 activation. To measure the level of cleaved caspase 3, cells were fixed with 75% (v/v) ethanol in PBS, permeabilized with 0.25% (v/v) Tween 20 in PBS and stained overnight with a rabbit antiserum specific for active Caspase-3 coupled with the fluorochrome FITC (FITC Rabbit Anti-Active Caspase-3, Clone C92-605 #559341, BD Biosciences). The FITC is measured with an excitation wavelength of 488 nm (blue laser) and an emission wavelength of 530 nm.

7/ Measurement of cleaved PARP. To measure the level of cleaved PARP, cells were fixed with 75% (v/v) ethanol in PBS, permeabilized with 0.25% (v/v) Tween 20 in PBS and stained overnight with a rabbit antiserum specific for cleaved PARP (Rabbit anti PARP cleaved (Y34), #ab32561, Abcam). Alexa Fluor® Plus 488 conjugated goat anti-rabbit was used as secondary antibody (Thermo fisher #A32731). The fluorescence is measured with an excitation wavelength of 488 nm (blue laser) and an emission wavelength of 530 nm.

Quantitative network mapping of the human kinome interactome

To perform the quantitative network mapping of the human kinome interactome we used STRING plugin related to the Cytoscape software. IC50 values were collected form STITCH database [28].

Heatmap of drugs efficiency

Heatmap of drugs efficiency on kinases panel was performed by gplots package on R.

Synergistic activity determination

CompuSyn version 1.0 software was used to evaluate the potential synergistic effect of Bi2536 in combination with paclitaxel, vincristine or colchicine where a combination index (CI) <1 indicated synergism, CI=1 additive effect and CI>1 antagonism.

Statistical analyses

Statistical analyses were performed using the GraphPad Software and assessed by non-parametric ANOVA (Mann-Whitney-test). The results are expressed as means ± standard deviation.

Results

Preferential killing of tetraploid cells after PLK1 inhibition

To evaluate the differential impact of PLK1 knockdown on the survival of tetraploid and diploid colon cancer cells, we utilised previously generated 2n and 4n clones derived from parental human colon carcinoma RKO cells [29]. The diploid and tetraploid clones were transfected with an unrelated small interfering RNA (siUNR) as a control and a SMARTpool siPLK1 (siPLK1a), to knockdown PLK1, for up to 72 h (Fig. 1A). The cells were fixed and stained with propidium iodide (PI) to assess with flow cytometry the cell cycle distribution and the proportion of the hypodiploid ($subG_1$) fraction, a hallmark of cell death (Fig. 1B). Compared to their diploid counterparts, tetraploid clones were particularly sensitive to PLK1 knockdown. In order to avoid any off-target activity of the siPLK1a, we used two additional siRNA: siPLK1b and siPLK1c. The knockdown efficiency for the three siRNAs was evaluated using real-time polymerase chain reaction (PCR), 48 h post-transfection (Fig. 1C). We performed a proliferation assay using crystal violet and found that tetraploid cells were more sensitive to PLK1 knockdown compared to their diploid counterpart (Fig. 1D-F). To further confirm our finding, the cells were transfected with siPLK1a, b or c and evaluated cell death after 72 h by co-staining with the vital dye propidium iodide (PI) and the mitochondrial transmembrane potential ($\Delta \psi m$) sensor $DiOC_6(3)$. The PI cell incorporation shows loss of cell membrane integrity and in consequence cell death ((DiOC6(3) low PI high), while loss of mitochondrial transmembrane potential (DiOC6(3)low PI low) is a sign of early stage apoptosis. The frequency of (DiOC6(3) low PI low) and (DiOC6(3)low PI high) cells analyzed by flow cytometry was indeed higher in tetraploid comparatively to diploid cells (Fig. 1G-H). The cell death mediated by PLK1 knockdown in tetraploid cells was also confirmed using human colon carcinoma HCT116 (Supplementary Fig. S1A-B) and sarcoma cells (Supplementary Fig. S2A – for all supplemental material see www.cellphysiolbiochem.com).

Next, we focused on small molecule PLK1inhibitors to assess a potentially alternative treatment option to target PLK1 for cancer therapy. We decided to focus on drugs that are already in clinical trials (Table 1). We performed a kinase-drug interaction network using the STRING plugin, which is related to the Cytoscape software [30], to extract the half maximal inhibitory concentration (IC_{50}) sensitivity of PLK1 of the listed drugs in Table 1 (Supplementary Fig. S3A-B). Among all the enumerated molecules, Bi2536 and GSK461364 showed the highest potency to inhibit PLK1 based on the IC_{50} values (Supplementary Fig. S3B). We utilised the KINOMEscan library, an online biochemical kinase profiling assay that measures drug binding using a panel of 309 purified kinases (https://lincs.hms.harvard.edu/kinomescan/). Based on the values obtained from the KINOMEscan library using

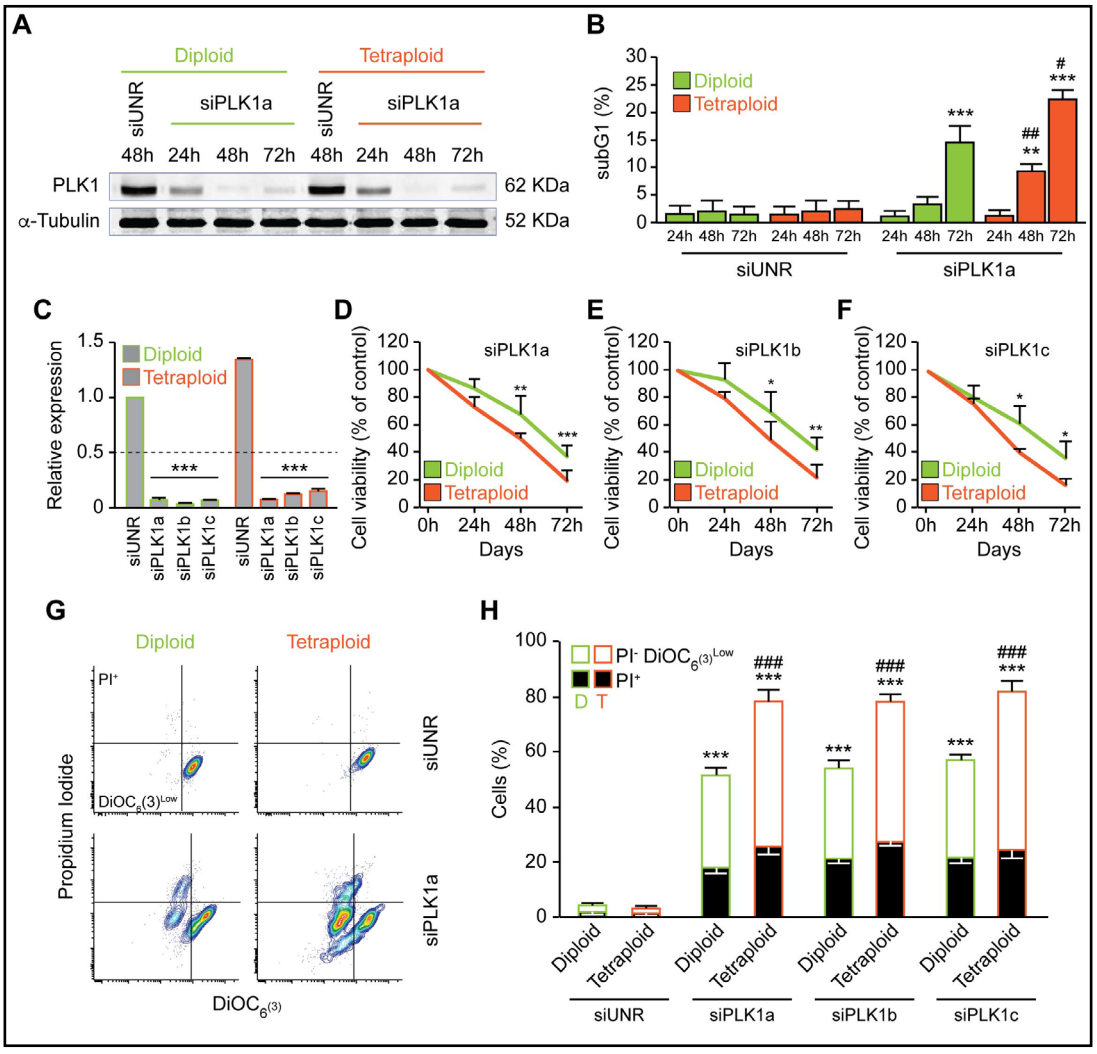

Fig. 1. Preferential killing of tetraploid cells after PLK1 knockdown. A. Diploid (labelled in green) and tetraploid (labelled in orange) human colorectal carcinoma cells were transfected with an unrelated small interfering RNA (siUNR) or a SMARTpool siPLK1 (siPLKa). After 24, 48 or 72 h, the cells were collected and lysed before a western blot analysis using antibodies directed against PLK1 and α-tubulin as a loading control. B. Alternatively, cells were subjected to the determination of DNA degradation following the cell cycle subG$_1$ population as a hallmark of cell death by flow cytometry upon cell fixation and propidium iodide (PI) staining. C. The knockdown efficiency of PLK using real-time polymerase chain reaction (PCR) in diploid and tetraploid RKO cells transfected with siUNR or three different siPLK1 (siPLK1a, siPLK1b and siPLK1c) for 48 h. D-F. Cell proliferation and death in cells transfected with siUNR or three different siPLK1 (siPLK1a, siPLK1b and siPLK1c) was examined after 72 h using a crystal violet assay. G-H. The cells were transfected with siUNR orthree different siPLK1 and co-stained with the vital dye PI and the mitochondrial membrane potential (Δψm)-sensing dye DiOC$_6$(3) to evaluate cell-death-associated parameters by cytofluorometry. A representative histogram of RKO diploid and tetraploid cells transfected with siUNR vs siPLK1a is shown in (G), while quantitative data are represented in (H). The white and black columns depict the percentage of dying (PI–DiOC$_6$(3)low) and dead (PI+) cells, respectively. Data are reported as means ± SD (n ≥ 3). ***p<0.001, **p<0.01, *p<0.05 (Mann–Whitney test), as compared to the control. ###p<0.001, ##p<0.01, #p<0.05 (Mann–Whitney test), as compared to diploid subjected to the same treatment condition.

Table 1. List of PLK1 inhibitors in clinical trial studies. * Lipid nanoparticle formulation of siRNA directed against Plk1. ** Prodrug of HMN-176 with improved oral absorption

PLK inhibitors	Commercial name	Target	Company	Clinical trial phase	Tumor type	Reference
BI6727	Volasertib	ATP-binding domain	Boehringer-Ingelheim	Phase 3	Solid tumors & Leukemia	68
ON-01910	Rigosertib	Plk1 non-competitive	Onconova Therapeutics	Phase 3	Solid tumors & Leukemia	69
BI2536		ATP-binding domain	Boehringer-Ingelheim	Phase 2	Solid tumors	70
TKM-080301 *		Plk1 non-competitive	Tekmira Pharmaceuticals Corporation	Phase 2	Solid tumors	71
GSK461364	GSK461364A	ATP-binding domain	GlaxoSmithKline	Phase 1	Solid tumors	72
NMS-P937	Onvansertib	ATP-binding domain	Nerviano Medical Science	Phase 2	Solid tumors & Leukemia	73
TAK-960		ATP-binding domain	Takeda Pharmaceuticals	Phase 1	Leukemia	74
HMN-214 **		ATP-binding domain	Nippon Shinyako	Phase 1	Solid tumors	75
CYC140		ATP-binding domain	Cyclacel Pharmaceuticals	Phase 1	Leukemia	76

Bi2536 and GSK461364 at 10 μM, we generated a heatmap of the drugs' specificity. The results for each inhibitor are reported as "percent of control", where the control is dimethyl sulphoxide (DMSO). A value of 100% indicated no inhibition of kinase binding to the ligand in the presence of Bi2536 or GSK461364, while a low percent indicated strong inhibition. Since Bi2536 was more specific for PLK1 compared to GSK461364 (Supplementary Fig. S3C), we decided to continue our investigation on tetraploid cells using Bi2536.

We initially performed a concentration dependent proliferation assay using crystal violet. The tetraploid cells showed a higher sensitivity against Bi2536-treatment after 24–72 h compared to diploid cells (Fig. 2A-C). The major differences in the Bi2536 was observed after 72 h (Fig. 2C). Tetraploid RKO cells treated with Bi2536 were more cytotoxic measuring the subG1 cell population compared to diploid cells (Fig. 2D). Moreover, using flow cytometry-mediated measurement of PI and $DiOC_6(3)$, tetraploid cells showed a higher sensitivity when treated with 5, 10 or 50 nM Bi2536 compared to diploid cells (Fig. 2E). Consistently, Bi2536 significantly reduced the clonogenic potential of tetraploid compared to diploid cells, either with continuous 5 nM Bi2536 treatment (75.3 +/- 25 diploid *vs* 4.3 +/- 3 tetraploid) or after 24 h drug washout (217 +/- 37 diploid *vs* 148 +/- 35 tetraploid) (Fig. 2F-G). The preferential toxicity of the Bi2536 to tetraploid cells was also confirmed using the human colon carcinoma HCT116 (Supplementary Fig. S1C-D) and sarcoma (Supplementary Fig. S2B) cells lines. Taken together, these findings demonstrated that targeting PLK1 represents an efficient strategy to preferentially kill tetraploid colon cancer cells.

The PLK1 inhibition triggered the mitochondrial apoptotic pathway in tetraploid colon cancer cells

To characterise the cell death pathway engaged after PLK1 inhibition, tetraploid RKO colon cancer cells were treated for 72 h with DMSO (as a control) or 10 nM Bi2536. Cell death was evaluated by flow-cytometry-mediated measurement of well-recognised apoptotic parameters [31], including phosphatidylserine (PS) surface exposure using Annexin V staining (Fig. 3A), dissipation of the mitochondrial inner transmembrane potential ($\Delta\psi m$) with the sensitive dye $DiOC_6(3)$ (Fig. 3B), examining the intracellular calcium (Ca^{2+}) concentration with the Fluo-3/AM dye (Fig. 3C) and caspase-3 cleavage with an appropriate

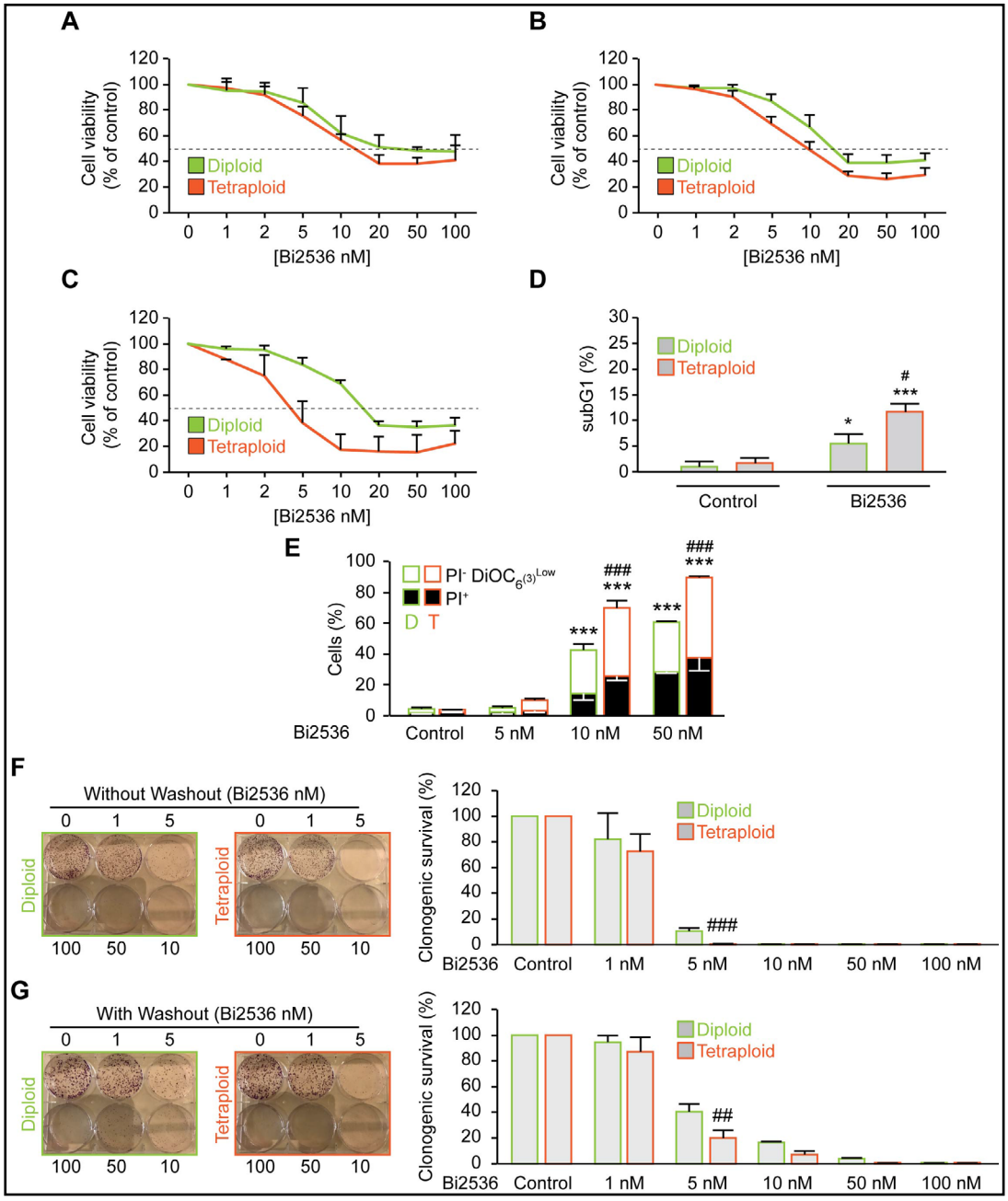

Fig. 2. Preferential killing of tetraploid cells after PLK1 chemical inhibition. A-C. Diploid and tetraploid RKO cells were exposed to DMSO control or increasing doses of the PLK1 inhibitor Bi2536 for 24 h (A), 48 h (B), or 72 h (C) before analysis with a crystal violet assay. D. Diploid and tetraploid RKO cells were treated with DMSO or 10 nM Bi2536. The subG$_1$ cell population was detected by flow cytometry upon fixation and propidium iodide (PI) staining after 72 h treatment. E. Diploid and tetraploid RKO cells were treated with DMSO or 5, 10 or 50 nM Bi2536 for 72 h before co-staining with PI and the mitochondrial membrane potential (Δψm)-sensing dye DiOC$_6$(3) for the evaluation of cell death by cytofluorometry. The white and black columns depict the percentage of dying (PI–DiOC$_6$(3)low) and dead (PI+) cells, respectively. F-G. Diploid and tetraploid RKO cells were seeded at low concentration for a clonogenic assay. The cells were treated with DMSO as a control or 1, 5, 10, 50 or 100 nM Bi2536 and cultivated for 15 days, without (F) or with a 24 h drug washout (G) before crystal violet staining and colony counting. Representative images for each condition are showed in panel and quantitative data of clonogenic survival comparatively to control are represented. Data are reported as means ± SD (n ≥ 3). ***p<0.001, **p<0.01, *p<0.05 (Mann–Whitney test), as compared to the control. ###p<0.001, ##p<0.01, #p<0.05 (Mann–Whitney test), as compared to diploid subjected to the same treatment condition.

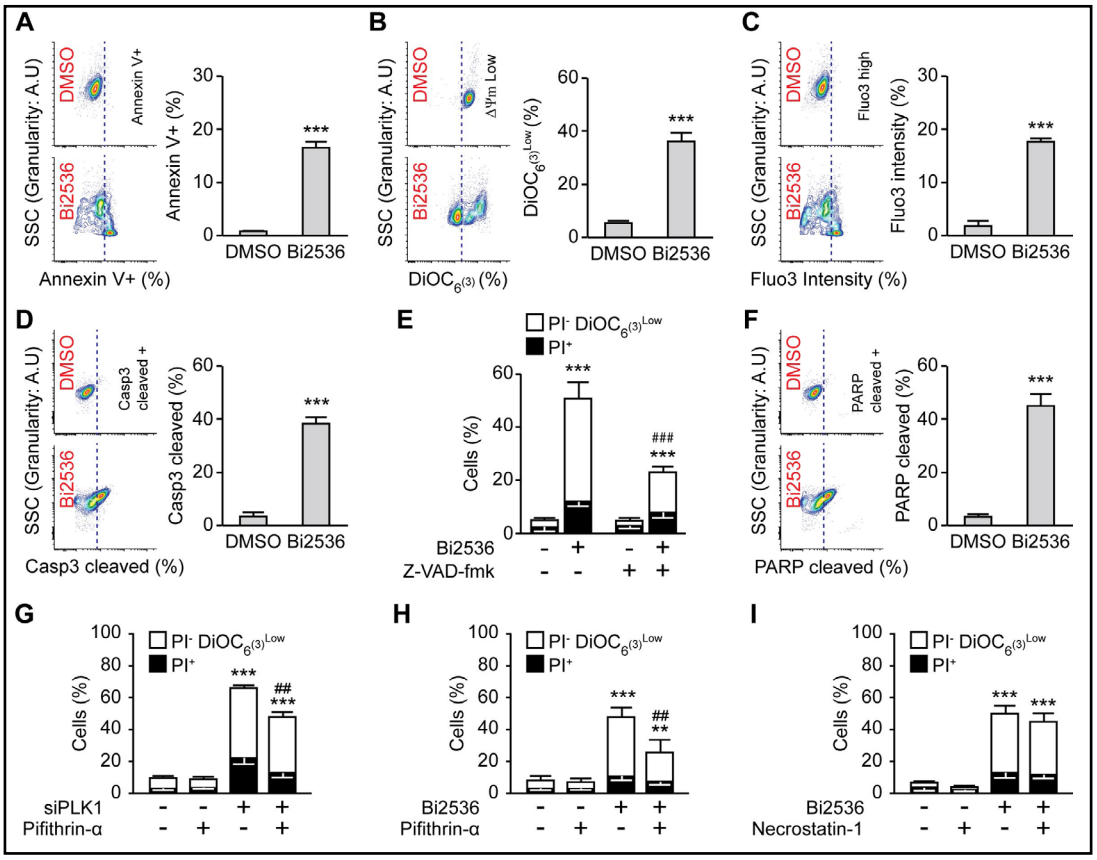

Fig. 3. PLK1 inhibition killed tetraploid colon cancer cells via the intrinsic apoptotic pathway. A. Tetraploid RKO cells were seeded before treating with DMSO or 10 nM Bi2536. After 72 h, the cells were collected and stained with FITC-conjugated Annexin V and analysed by flow cytometry for the detection of phosphatidylserine exposure. Representative dot plots are presented in the left panel, and quantitative data are presented in the right panel. B. The cells were stained with the mitochondrial membrane potential (Δψm)-sensing dye $DiOC_6(3)$. Representative dot plots (left panel) and quantitative data (right panel) of the signal shift of DMSO and Bi2536 treated cells are represented. C. The cells were stained with the calcium dye Fluo-3 to quantify the cytosolic Ca^{2+} concentration by flow cytometry. Representative dot plots of DMSO and Bi2536 treated cells are showed and quantitative data of the signal shift are represented. D. The cells were fixed with cold 75% ethanol and labelled with the FITC-conjugated Casp3 c to detect cleaved caspase-3 by flow cytometry. Representative dot plots of DMSO and Bi2536 treated cells are shown, and quantitative data of the signal shift are represented. E. The effects of the pan caspase inhibitor Z-VAD-fmk on PLK1-inhibitor-induced cell death. Tetraploid RKO cells were treated for 72 h with the PLK1 inhibitor alone or in combination with 50 µM Z-VAD-fmk, followed by $DiOC_6(3)$/PI co-staining. The white and black columns depict the percentage of dying (PI–$DiOC_6(3)$ low) and dead (PI+) cells, respectively. F. The cells were fixed with cold 75% ethanol and labelled with a cleaved PARP antibody to detect cleaved PARP by flow cytometry. Representative dot plots of DMSO- and Bi2536-treated cells are shown, and quantitative data of the signal shift are represented. G. The effects of the p53 antagonist pifithrin-α (PFT-α) on PLK-knockdown-induced cell death. Tetraploid RKO cells were transfected with siUNR or siPLK1 for 72 h alone or in combination with 20 ng/ml PFT-α followed by $DiOC_6(3)$/PI co-staining. Quantitative data are represented. The white and black columns depict the percentage of dying (PI–$DiOC_6(3)$ low) and dead (PI+) cells, respectively. H. The effects of the p53 antagonist PFT-α on Bi2536-induced cell death. Tetraploid RKO cells were treated for 72 h with Bi2536 alone or in combination with 20 ng/ml PFT-α followed by $DiOC_6(3)$/PI co-staining. Quantitative data are represented. The white and black columns depict the percentage of dying (PI–$DiOC_6(3)$ low) and dead (PI+) cells, respectively. I. The effects of the necroptosis inhibitor necrostatin-1 on PLK1-inhibitor-induced cell death. Tetraploid RKO cells were treated for 72 h with the PLK1 inhibitor alone or in combination with 100 µM necrostatin-1, followed by $DiOC_6(3)$/PI co-staining. Quantitative data are represented. The white and black columns depict the percentage of dying (PI–$DiOC_6(3)$ low) and dead (PI+) cells, respectively. Data are reported as means ± SD (n ≥ 3). ***p<0.001, **p<0.01 (Mann–Whitney test), as compared to the control. ###p<0.001, ##p<0.01 (Mann–Whitney test), as compared to diploid subjected to the same treatment condition.

antibody (Fig. 3D). Moreover, the co-treatment of the cells with the broad-spectrum caspase inhibitor Z-Val-Ala-Asp-fluoromethylketone (Z-VAD-fmk) significantly reduced the death of tetraploid cells that responded to PLK1 inhibition (Fig. 3E). Further confirming the role of caspases in the execution of apoptosis, tetraploid cells that responded to Bi2536 manifested the apoptosis-associated cleavage of poly (ADP-ribose) polymerase (PARP) (Fig. 3F). These results indicated that PLK1 inhibition triggers the intrinsic pathway of apoptosis in tetraploid colon cancer cells.

P53 is the most frequently mutated gene in human cancers [32]. Moreover, p53 is the major mediator of the cellular response to stress, and it stimulates the execution of apoptosis via the transactivation of several proapoptotic genes [33]. Thus, we investigated the effect of p53 inhibition when PLK1 was knocked down or inhibited by treating the tetraploid RKO cells with cyclic pifithrin-α (PFT-α), a pharmacological antagonist of p53 [34], in the presence of siPLK1 (Fig. 3G) and with Bi2536 co-treatment (Fig. 3H). Cell death was assessed by flow cytometry by co-staining with the mitochondrial inner transmembrane potential (Δψm) sensitive dye $DiOC_6(3)$ and the vital dye PI. This procedure identifies dying cells ($DiOC_6(3)$ low PI−) and dead (PI+) cells. The loss of p53 function conferred a death resistance to the treatment (Fig. 3G-H). To investigate the effect of PLK1 inhibition on necroptosis induction, the cells were co-treated with 10 nM Bi2536 and 100 µM of the necroptosis inhibitor necrostatin-1. There was no protective effect after co-staining with $DiOC_6(3)$ and PI, a finding that excluded any role of PLK1 inhibition to induce regulated necrosis (Fig. 3I).

Targeting PLK1 perturbed tetraploid cell cycle divisions

When analysing cell cycle profiles using flow cytometry after staining fixed cells with the DNA dye PI, we observed that inhibition or depletion of PLK1 perturbed the diploid

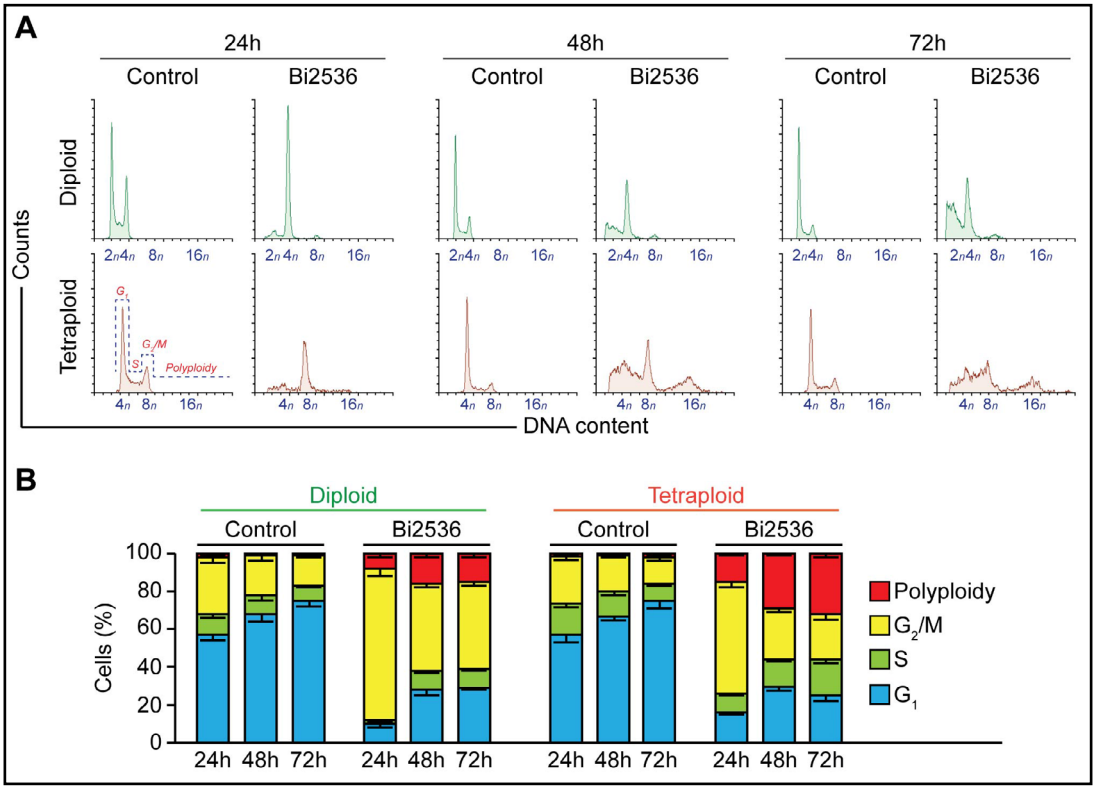

Fig. 4. PLK1 inhibition perturbed the cell cycle. A-B. Diploid and tetraploid human colorectal carcinoma RKO cells were treated with DMSO or 10 nM Bi2536. After 24, 48 or 72 h, the cells were collected and fixed with cold 75% ethanol. The fixed cells were further labelled with propidium iodide (PI), followed by the assessment of cell cycle distribution. A representative histogram and quantitative data are represented.

and tetraploid cell cycle progression. We excluded the subG$_1$ population to focus on the proliferative cells (Fig. 4A). Compared to the control conditions, the cells were blocked in G2/M phase after 24 h treatment. Some cells underwent mitotic slippage and became hyper-diploid and hyper-tetraploid, respectively. (Hyperploidy is shown in the figure as DNA content > 4*n* and > 8*n* for diploid and tetraploid clones, respectively). Notably, the fraction of hyperploidisation induced by PLK1 inhibition was higher in tetraploid compared to diploid cells (Fig. 4B). Indeed, the diploid cells stayed in the G2/M phase longer than tetraploid cells, and approximately 15% of the cells became hyper-diploid after 72 h. However, tetraploid cells executed mitotic slippage earlier; the hyperploid fraction was approximately 16% at 24 h and reached 32% at 72 h. These findings suggest that the anti-tetraploid effect of PLK1 inhibition came from the relative inability of tetraploid (as compared to diploid) cells to tolerate any further increase in ploidy. Targeting PLK1 preferentially kills tetraploid colon cancer cells by triggering an uncontrolled and lethal hyperploidisation programme, followed by a mitotic catastrophe executed by the intrinsic apoptotic pathway.

PLK1 and tubulin polymerisation inhibitors synergistically induced apoptosis in tetraploid colon cancer cells

Given that PLK1 inhibition induced mitotic catastrophe and polyploidy after a long arrest in the mitotic phase, we asked whether the combination of PLK1 inhibition with a microtubule poison could promote any synergistic effects concerning cells death in tetraploid colon cancer cells. To address this question, we used different classes of microtubules poisons, including paclitaxel as a tubulin depolymerisation inhibitor and vincristine or colchicine as tubulin polymerisation inhibitors. We found a concentration dependent cell survival in tetraploid cells. (Fig. 5A, 5C and Supplementary Fig. S4A). The combination of Bi2536 and paclitaxel did not result in any synergistic activity (Supplementary Fig. S4B-C

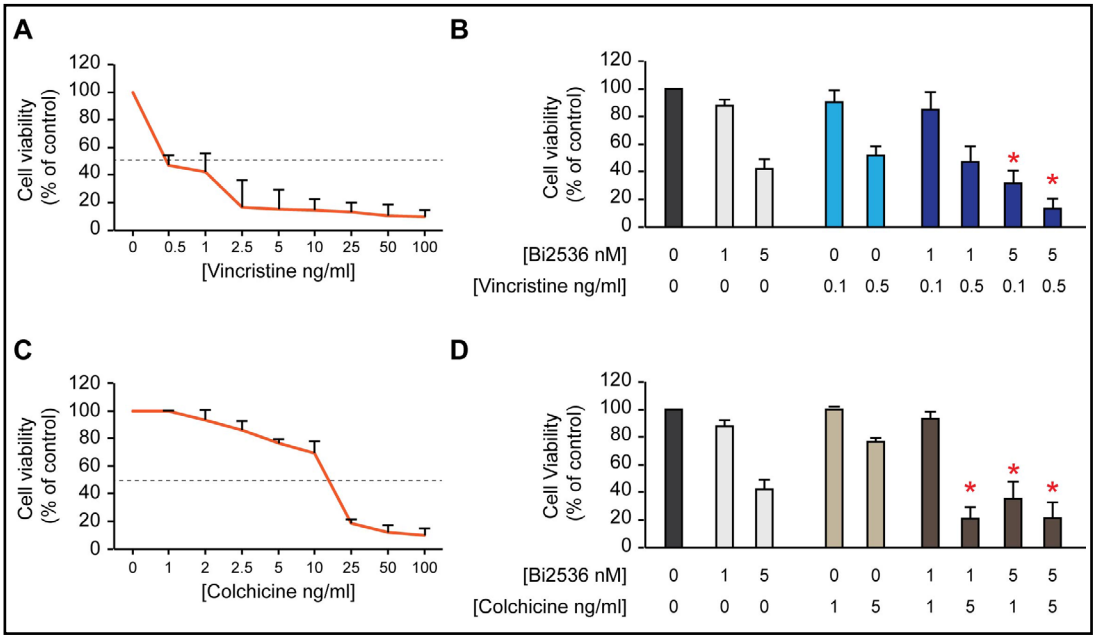

Fig. 5. Synergistic lethality of low-dose PLK1 inhibitor and microtubule polymerisation inhibitors. A. Tetraploid RKO cells were exposed to different doses of vincristine and cell survival was calculated after 72 h using a crystal violet assay. B. Tetraploid RKO cells were treated with different concentrations of Bi2536 and vincristine to evaluate the synergetic effect of the combination treatment. The red stars indicate the synergetic effect of the treatment condition. C. Tetraploid RKO cells were exposed to increased dose of colchicine and cell survival was calculated at 72 h using crystal violet assay. D. Combination treatment with Bi2536 and colchicine was performed to evaluate the synergetic effect of the combination treatment. The red stars indicate a synergetic effect for the treatment condition.

and Table 2), whereas the combination of Bi2536 and vincristine or colchicine provoked significant synergy in the cell survival (Fig. 5B, 5D and Table 2). Taken together, these data underscore the possibility of combining PLK1 and microtubule polymerisation inhibition but not microtubule depolymerisation agent for the treatment for colorectal cancer.

Table 2. Synergistic measurement of drugs combination

Concentration		Growth Inhibition	CI
Paclitaxel (nM)	Bi2536 (nM)		
0,00	0,00	0%	-
0,10	0,00	21%	-
0,50	0,00	65%	-
1,00	0,00	69%	-
0,00	1,00	13%	-
0,10	1,00	12%	3,23587
0,50	1,00	63%	1,00555
1,00	1,00	65%	1,66724
0,00	5,00	62%	-
0,10	5,00	59%	1,28109
0,50	5,00	68%	1,48306
1,00	5,00	70%	1,95961
Vincristine (ng/ml)	Bi2536 (nM)		
0,00	0,00	0%	-
0,10	0,00	10%	-
0,50	0,00	48%	-
0,00	1,00	12%	-
0,10	1,00	15%	1,53942
0,50	1,00	53%	1,08909
0,00	5,00	58%	-
0,10	5,00	68%	0,84721
0,50	5,00	87%	0,55565
Colchicine (ng/ml)	Bi2536 (nM)		
0,00	0,00	0%	-
1,00	0,00	0%	-
5,00	0,00	23%	-
0,00	1,00	12%	-
1,00	1,00	7%	1,80669
5,00	1,00	79%	0,58861
0,00	5,00	58%	-
1,00	5,00	65%	0,93324
5,00	5,00	79%	0,98721

Discussion

In this study, we proposed a novel strategy for targeting tetraploid colon cancer cells based on the abrogation of the mitotic kinase PLK1. By using tumour cells that display distinct levels of ploidy (diploid and tetraploid), we showed that the depletion or inhibition of PLK1 effectively and preferentially killed tetraploid colon cancer cells *via* mitotic catastrophe and the activation of a mitochondrial- and caspase-dependent apoptosis. The cell death mechanism occurred after a G2/M block, followed by mitotic slippage and polyploidy. In addition, we provided evidence that the combination of PLK1 inhibition with microtubule polymerisation inhibitors (vincristine or colchicine) induced significant synergetic cell death (Fig. 6).

PLK1 is the most investigated member of the PLK serine/threonine protein kinases family [24, 27]. During the cell cycle, PLK1 controls, among others, mitotic entry and the G2/M checkpoint, coordinates the centrosome cycle, regulates the chromosome segregation, plays multiple functions at the spindle midzone, participates in abscission and is involved in cytokinesis [24, 25, 35, 36]. In the Cancer Genome Atlas (TCGA) database (https://tcga-data.nci.nih.gov/tcga/), PLK1 messenger RNA (mRNA) expression is significantly higher in tumour compared to normal tissue (across 24 different types of cancers). In comparison to other cancer types, colorectal cancer exhibits high PLK1 expression [26]. Moreover, a previous study showed that upregulated PLK1 expression correlates with inferior survival outcomes in patients with rectal cancer [37]. PLK1 overexpression induces chromosomal instability [38], a finding that places this kinase as a promising antineoplastic target for cancers with a high level of genomic instability, especially colorectal tumours.

The Bi2536 inhibitor is the most commonly molecule used in the characterisation of PLK1 function and anticancer activity [39]. Bi2536 is a well-tolerated inhibitor with potent efficacy *in vivo*, in several well-established xenograft models [40]. Moreover, Bi2536 was included in a completed phase II clinical trial for patients with solid tumours, including non-small cell lung, pancreatic or hormone-refractory prostate cancer (clinicaltrials.gov, NCT00376623, NCT00706498, NCT00412880 and NCT00710710). However, we have not identified any PLK1 inhibitor that has entered the chemotherapeutic market.

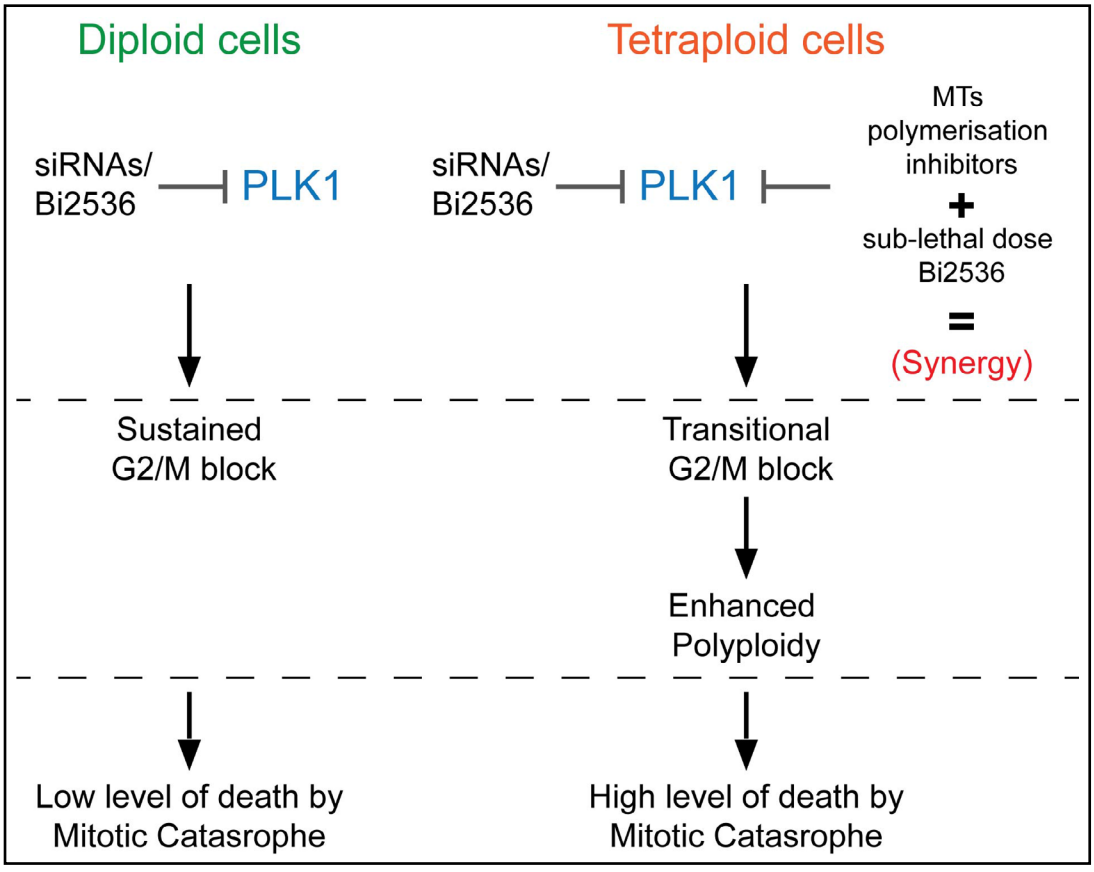

Fig. 6. Schematic summary. A schematic summary of PLK1 inhibition that shows a preferential fate in diploid versus tetraploid cells.

In our experimental model, either depletion or chemical inhibition of PLK1 provoked apoptosis in both diploid and tetraploid colon cells. However, tetraploid cells showed higher sensitivity when PLK1 was targeted. Tetraploid cell death was executed via the intrinsic apoptotic pathway, as demonstrated by the loss of mitochondrial transmembrane potential (Δψm), accumulation of intracellular calcium, activation of caspase-3 and PARP, DNA degradation, cell scrambling, phosphatidylserine (PS) exposure and, ultimately, the loss of plasma membrane integrity. The mitochondrial dysfunction, measured by the loss of the mitochondrial membrane potential, provokes a mitochondrial Ca^{2+} homeostasis perturbation. This leads to elevated cytosolic Ca^{2+} concentration ([Ca2+]c), which is followed by the release of mitochondrial apoptotic factors, including cytochrome c, apoptosis inducing factor (AIF) and procaspase-9, into the cytosol [41]. The PLK1 inhibition perturbed cell mitosis and provoked instead mitotic catastrophe. This in turn facilitated a *bona fide* intrinsic oncosuppressive mechanism that by sensing mitotic failure, executed cell death *via* the mitochondrial pathway of apoptosis.

What is the mechanism through which PLK1 inhibition is particularly lethal for tetraploid cells? To answer this question, we monitored the cell cycle status upon PLK1 inhibition. This inhibition prolonged G2/M arrest in diploid cells for up to 72 h, followed by mitotic slippage for approximately 15% of the cell population. The tetraploid cells responded similarly, but with completely different kinetics. The length of the G2/M arrest was significantly shorter, and the polyploid population reached almost 30% 48 h post-PLK1 inhibition. It appeared that tetraploid cells death upon PLK1 inhibition was caused by excessive genome reduplication and consequent hyperploidy as well as their incapacity to support accumulation of additional DNA content.

Our findings are consistent with previous studies showing that the high sensitivity of tetraploid cells to the inhibition of mitotic key effectors, especially those with a direct interaction with microtubules. Inhibition of the protein kinase Aurora B preferentially kills tetraploid compared to diploid hepatocellular carcinoma cells, but it also shows a similar effect on untransformed tetraploid *vs* diploid mouse fibroblasts. This effect is due to a cytokinesis failure, consequent massive polyploidy and subsequent mitotic catastrophe [42]. Aurora B interacts with a key kinase of the SAC, namely MPS1 [43-45]. MPS1 inhibition sensitises the tetraploid colon cancer cells also *via* the activation of the mitotic catastrophe following a polyploid/aneuploid cascade [46, 47]. It is important to note that PLK1 and MPS1 cooperatively regulate the SAC [48]. The protein kinase CHK1 is an important component of DNA damage pathway; however, it also plays an essential role in the SAC function via the activation of Aurora B and MAD2 [49]. CHK1 loss leads to chromosome misalignment and lagging chromosomes and thus preferential killing of tetraploid colon cancer cells [50]. Other players involved in microtubule dynamics and essentially centrosome separation and pole formation are kinesin Eg5 and the protein motor HSET. The inhibition/depletion of these proteins also sensitises and preferentially kills tetraploid compared to diploid colon cancer cells after mitotic catastrophe activation [51, 52]. We must emphasise that not all the SAC components or important players of the microtubule dynamics can preferentially sensitise the tetraploid cancer cells. The inhibition of Aurora A, an important kinase for centrosome maturation, mitotic spindle formation and cytokinesis, does not kill tetraploid hepatocellular carcinoma [42, 53].

Drug combinations are particularly important in the modern era of chemotherapy; they offer the advantage of synergistic antitumor activity at relatively low concentrations of each drug and reduce side effects and additive toxicity. Moreover, compound synergy might overcome the drug resistance of certain tumours, including cancers that harbour chromosomal instability and particularly tetraploidy, which is highly correlated with drug resistance and a poor patient prognosis [20, 54-56]. Due to the key role of PLK1 in several cell cycle processes, including centrosome maturation, bipolar spindle formation and kinetochore-microtubule attachment, we asked whether there is a lethal interaction between PLK1 inhibition and microtubule-destabilising drugs to induce apoptosis. There are two types of microtubule poisons widely used in chemotherapy: microtubule depolymerisation and polymerisation inhibitors [57, 58]. Paclitaxel (commonly named Taxol) is the most utilised microtubule depolymerisation inhibitor in preclinical and clinical models [59]. Microtubule polymerisation inhibitors, including vincristine from the Vinca alkaloid group [60] and the colchicine from the Colchicine group, are more diverse [61].

We found that co-treatment with a low dose of the PLK1 inhibitor Bi2536 and paclitaxel did not induce any synergistic lethality in tetraploid colon cancer cells. On the other hand, co-treatment of a low dose of the PLK1 inhibitor Bi2536 and a low dose of either vincristine or colchicine induced strong synergistic toxicity in tetraploid colon cancer cells. These findings are consistent with previous studies that employed vincristine in combination with PLK1 inhibitors for the treatment of various solid tumours and haematological malignancies [62-67]. Our study is the first report to use colchicine as an effective treatment strategy in combination with PLK1 inhibition.

Conclusion

In conclusion, this novel approach to exploit PLK1 inhibitors and microtubule poisons constitutes a promising therapeutic strategy based on mitotic catastrophe for colon cancer.

Acknowledgements

This work was supported by the Wenner-Gren Foundation (UPD2018-0055) and by funding from Per-Eric and Ulla Schyberg's Foundation (39178), Gunnar Nilssons Cancerstiftelse (GN-2019-2-137), The Crafoord Foundation (20190584), the Sigurd och Elsa Goljes Minne Foundation (LA2018-0168) and the Royal Physiographic Society of Lund (39448).

Author contributions statements

MJ developed the concepts and performed experiments. CK performed the bio-informatics work and statistical analysis. SSS performed experiments. MJ and RM analyzed data and wrote the manuscript. All authors reviewed the manuscript.

Disclosure Statement

The authors declare no conflict of interests.

References

1 Kolligs FT: Diagnostics and Epidemiology of Colorectal Cancer. Visc Med 2016;32:158-164.
2 Arnold M, Sierra MS, Laversanne M, Soerjomataram I, Jemal A, Bray F: Global patterns and trends in colorectal cancer incidence and mortality. Gut 2017;66:683-691.
3 Swanton C: Intratumor heterogeneity: evolution through space and time. Cancer Res 2012;72:4875-4882.
4 Potapova TA, Zhu J, Li R: Aneuploidy and chromosomal instability: a vicious cycle driving cellular evolution and cancer genome chaos. Cancer Metastasis Rev 2013;32:377-389.
5 Vitale I, Galluzzi L, Senovilla L, Criollo A, Jemaa M, Castedo M, Kroemer G: Illicit survival of cancer cells during polyploidization and depolyploidization. Cell Death Differ 2011;18:1403-1413.
6 Storchova Z, Kuffer C: The consequences of tetraploidy and aneuploidy. J Cell Sci 2008;121:3859-3866.
7 Ganem NJ, Storchova Z, Pellman D: Tetraploidy, aneuploidy and cancer. Curr Opin Genet Dev 2007;17:157-162.
8 Davoli T, de Lange T: The causes and consequences of polyploidy in normal development and cancer. Annu Rev Cell Dev Biol 2011;27:585-610.
9 Davoli T, Denchi EL, de Lange T: Persistent telomere damage induces bypass of mitosis and tetraploidy. Cell 2010;141:81-93.
10 Fujiwara T, Bandi M, Nitta M, Ivanova EV, Bronson RT, Pellman D: Cytokinesis failure generating tetraploids promotes tumorigenesis in p53-null cells. Nature 2005;437:1043-1047.
11 Ganem NJ, Cornils H, Chiu SY, O'Rourke KP, Arnaud J, Yimlamai D, Thery M, Camargo FD, Pellman D: Cytokinesis failure triggers hippo tumor suppressor pathway activation. Cell 2014;158:833-848.
12 Duelli DM, Padilla-Nash HM, Berman D, Murphy KM, Ried T, Lazebnik Y: A virus causes cancer by inducing massive chromosomal instability through cell fusion. Curr Biol 2007;17:431-437.
13 Svendsen LB, Thorup J, Larsen JK, Bulow S, Horn T: Correlation between in vitro tetraploidy in skin fibroblasts and development of sporadic colorectal carcinomas. Cancer Genet Cytogenet 1990;50:139-148.
14 Boileve A, Senovilla L, Vitale I, Lissa D, Martins I, Metivier D, van den Brink S, Clevers H, Galluzzi L, Castedo M, Kroemer G: Immunosurveillance against tetraploidization-induced colon tumorigenesis. Cell Cycle 2013;12:473-479.
15 Lissa D, Senovilla L, Rello-Varona S, Vitale I, Michaud M, Pietrocola F, Boileve A, Obrist F, Bordenave C, Garcia P, Michels J, Jemàa M, Kepp O, Castedo M: Resveratrol and aspirin eliminate tetraploid cells for anticancer chemoprevention. Proc Natl Acad Sci U S A 2014;111:3020-3025.
16 Senovilla L, Vitale I, Galluzzi L, Vivet S, Joza N, Younes AB, Rello-Varona S, Castedo M, Kroemer G: p53 represses the polyploidization of primary mammary epithelial cells by activating apoptosis. Cell Cycle 2009;8:1380-1385.

17 Aylon Y, Oren M: p53: guardian of ploidy. Mol Oncol 2011;5:315-323.
18 Caldwell CM, Green RA, Kaplan KB: APC mutations lead to cytokinetic failures in vitro and tetraploid genotypes in Min mice. J Cell Biol 2007;178:1109-1120.
19 Lee AJ, Endesfelder D, Rowan AJ, Walther A, Birkbak NJ, Futreal PA, Downward J, Szallasi Z, Tomlinson IP, Howell M, Kschischo M, Swanton C: Chromosomal instability confers intrinsic multidrug resistance. Cancer Res 2011;71:1858-1870.
20 Castedo M, Coquelle A, Vitale I, Vivet S, Mouhamad S, Viaud S, Zitvogel L, Kroemer G: Selective resistance of tetraploid cancer cells against DNA damage-induced apoptosis. Ann N Y Acad Sci 2006;1090:35-49.
21 Petronczki M, Lenart P, Peters JM: Polo on the Rise-from Mitotic Entry to Cytokinesis with Plk1. Dev Cell 2008;14:646-659.
22 Wang G, Jiang Q, Zhang C: The role of mitotic kinases in coupling the centrosome cycle with the assembly of the mitotic spindle. J Cell Sci 2014;127:4111-4122.
23 Zitouni S, Nabais C, Jana SC, Guerrero A, Bettencourt-Dias M: Polo-like kinases: structural variations lead to multiple functions. Nat Rev Mol Cell Biol 2014;15:433-452.
24 Colicino EG, Hehnly H: Regulating a key mitotic regulator, polo-like kinase 1 (PLK1). Cytoskeleton (Hoboken) 2018;75:481-494.
25 Combes G, Alharbi I, Braga LG, Elowe S: Playing polo during mitosis: PLK1 takes the lead. Oncogene 2017;36:4819-4827.
26 Cunningham CE, Li S, Vizeacoumar FS, Bhanumathy KK, Lee JS, Parameswaran S, Furber L, Abuhussein O, Paul JM, McDonald M, Templeton SD, Shukla H, El Zawily AM, Boyd F, Alli N, Mosseau DD, Geyer R, Bonham K, Anderson DH, Yan J, et al.: Therapeutic relevance of the protein phosphatase 2A in cancer. Oncotarget 2016;7:61544-61561.
27 de Carcer G: The Mitotic Cancer Target Polo-Like Kinase 1: Oncogene or Tumor Suppressor? Genes (Basel) 2019;10:pii:E208.
28 Szklarczyk D, Santos A, von Mering C, Jensen LJ, Bork P, Kuhn M: STITCH 5: augmenting protein-chemical interaction networks with tissue and affinity data. Nucleic Acids Res 2016;44:D380-384.
29 Castedo M, Galluzzi L, Vitale I, Senovilla L, Metivier D, Jemaa M, Rello-Varona S, Kroemer G: Cytofluorometric purification of diploid and tetraploid cancer cells. Methods Mol Biol 2011;761:47-63.
30 Doncheva NT, Morris JH, Gorodkin J, Jensen LJ: Cytoscape StringApp: Network Analysis and Visualization of Proteomics Data. J Proteome Res 2019;18:623-632.
31 Galluzzi L, Vitale I, Aaronson SA, Abrams JM, Adam D, Agostinis P, Alnemri ES, Altucci L, Amelio I, Andrews DW, Annicchiarico-Petruzzelli M, Antonov AV, Aram E, Baehrecke EH, Barlev NA, Bazan NG, Bernassola F, Bertrand MJM, Bianchi K, Blagosklonny MV, et al.: Molecular mechanisms of cell death: recommendations of the Nomenclature Committee on Cell Death 2018. Cell Death Differ 2018;25:486-541.
32 Hollstein M, Sidransky D, Vogelstein B, Harris CC: p53 mutations in human cancers. Science 1991;253:49-53.
33 Roos WP, Kaina B: DNA damage-induced cell death by apoptosis. Trends Mol Med 2006;12:440-450.
34 Komarov PG, Komarova EA, Kondratov RV, Christov-Tselkov K, Coon JS, Chernov MV, Gudkov AV: A chemical inhibitor of p53 that protects mice from the side effects of cancer therapy. Science 1999;285:1733-1737.
35 Joukov V, De Nicolo A: Aurora-PLK1 cascades as key signaling modules in the regulation of mitosis. Sci Signal 2018;11:pii:eaar4195.
36 Saurin AT: Kinase and Phosphatase Cross-Talk at the Kinetochore. Front Cell Dev Biol 2018;6:62.
37 Tut TG, Lim SH, Dissanayake IU, Descallar J, Chua W, Ng W, de Souza P, Shin JS, Lee CS: Upregulated Polo-Like Kinase 1 Expression Correlates with Inferior Survival Outcomes in Rectal Cancer. PLoS One 2015;10:e0129313.
38 de Carcer G, Venkateswaran SV, Salgueiro L, El Bakkali A, Somogyi K, Rowald K, Montanes P, Sanclemente M, Escobar B, de Martino A, McGranahan N, Malumbres M, Sotillo R: Plk1 overexpression induces chromosomal instability and suppresses tumor development. Nat Commun 2018;9:3012.
39 Gutteridge RE, Ndiaye MA, Liu X, Ahmad N: Plk1 Inhibitors in Cancer Therapy: From Laboratory to Clinics. Mol Cancer Ther 2016;15:1427-1435.
40 Steegmaier M, Hoffmann M, Baum A, Lenart P, Petronczki M, Krssak M, Gurtler U, Garin-Chesa P, Lieb S, Quant J, Grauert M, Adolf GR, Kraut N, Peters JM, Rettig WJ: BI 2536, a potent and selective inhibitor of polo-like kinase 1, inhibits tumor growth in vivo. Curr Biol 2007;17:316-322.

41 Giorgi C, Baldassari F, Bononi A, Bonora M, De Marchi E, Marchi S, Missiroli S, Patergnani S, Rimessi A, Suski JM, Wieckowski MR, Pinton P: Ca(2+) and apoptosis. Cell Calcium 2012;52:36-43.
42 Marxer M, Foucar CE, Man WY, Chen Y, Ma HT, Poon RY: Tetraploidization increases sensitivity to Aurora B kinase inhibition. Cell Cycle 2012;11:2567-2577.
43 Saurin AT, van der Waal MS, Medema RH, Lens SM, Kops GJ: Aurora B potentiates Mps1 activation to ensure rapid checkpoint establishment at the onset of mitosis. Nat Commun 2011;2:316.
44 van der Waal MS, Saurin AT, Vromans MJ, Vleugel M, Wurzenberger C, Gerlich DW, Medema RH, Kops GJ, Lens SM: Mps1 promotes rapid centromere accumulation of Aurora B. EMBO Rep 2012;13:847-854.
45 Jelluma N, Brenkman AB, van den Broek NJ, Cruijsen CW, van Osch MH, Lens SM, Medema RH, Kops GJ: Mps1 phosphorylates Borealin to control Aurora B activity and chromosome alignment. Cell 2008;132:233-246.
46 Jemaa M, Manic G, Lledo G, Lissa D, Reynes C, Morin N, Chibon F, Sistigu A, Castedo M, Vitale , Kroemer G, Abrieu A: Whole-genome duplication increases tumor cell sensitivity to MPS1 inhibition. Oncotarget 2016;7:885-901.
47 Jemaa M, Galluzzi L, Kepp O, Castedo M, Rello-Varona S, Vitale I, Kroemer G: Transgenerational cell fate profiling: a method for the graphical presentation of complex cell cycle alterations. Cell Cycle 2013;12:183-190.
48 von Schubert C, Cubizolles F, Bracher JM, Sliedrecht T, Kops G, Nigg EA: Plk1 and Mps1 Cooperatively Regulate the Spindle Assembly Checkpoint in Human Cells. Cell Rep 2015;12:66-78.
49 Lawrence KS, Engebrecht J: The spindle assembly checkpoint: More than just keeping track of the spindle. Trends Cell Mol Biol 2015;10:141-150.
50 Vitale I, Galluzzi L, Vivet S, Nanty L, Dessen P, Senovilla L, Olaussen KA, Lazar V, Prudhomme M, Golsteyn RM, Castedo M, Kroemer G: Inhibition of Chk1 kills tetraploid tumor cells through a p53-dependent pathway. PLoS One 2007;2:e1337.
51 Rello-Varona S, Vitale I, Kepp O, Senovilla L, Jemaa M, Metivier D, Castedo M, Kroemer G: Preferential killing of tetraploid tumor cells by targeting the mitotic kinesin Eg5. Cell Cycle 2009;8:1030-1035.
52 Kwon M, Godinho SA, Chandhok NS, Ganem NJ, Azioune A, Thery M, Pellman D: Mechanisms to suppress multipolar divisions in cancer cells with extra centrosomes. Genes Dev 2008;22:2189-2203.
53 Yan M, Wang C, He B, Yang M, Tong M, Long Z, Liu B, Peng F, Xu L, Zhang Y, Liang D, Lei H, Substrata S, Kelley KW, Lam EW, Jin B, Liu Q: Aurora-A Kinase: A Potent Oncogene and Target for Cancer Therapy. Med Res Rev 2016;36:1036-1079.
54 Mosieniak G, Sliwinska MA, Alster O, Strzeszewska A, Sunderland P, Piechota M, Was H, Sikora E: Polyploidy Formation in Doxorubicin-Treated Cancer Cells Can Favor Escape from Senescence. Neoplasia 2015;17:882-893.
55 Coward J, Harding A: Size Does Matter: Why Polyploid Tumor Cells are Critical Drug Targets in the War on Cancer. Front Oncol 2014;4:123.
56 Castedo M, Coquelle A, Vivet S, Vitale I, Kauffmann A, Dessen P, Pequignot MO, Casares N, Valent A, Mouhamad S, Schmitt E, Modjtahedi N, Vainchenker W, Zitvogel L, Lazar V, Garrido C, Kroemer G: Apoptosis regulation in tetraploid cancer cells. EMBO J 2006;25:2584-2595.
57 Long HJ: Paclitaxel (Taxol): a novel anticancer chemotherapeutic drug. Mayo Clin Proc 1994;69:341-345.
58 Kaur R, Kaur G, Gill RK, Soni R, Bariwal J: Recent developments in tubulin polymerization inhibitors: An overview. Eur J Med Chem 2014;87:89-124.
59 de Weger VA, Beijnen JH, Schellens JH: Cellular and clinical pharmacology of the taxanes docetaxel and paclitaxel--a review. Anticancer Drugs 2014;25:488-494.
60 Stanton RA, Gernert KM, Nettles JH, Aneja R: Drugs that target dynamic microtubules: a new molecular perspective. Med Res Rev 2011;31:443-481.
61 Mukhtar E, Adhami VM, Mukhtar H: Targeting microtubules by natural agents for cancer therapy. Mol Cancer Ther 2014;13:275-284.
62 Ikezoe T, Yang J, Nishioka C, Takezaki Y, Tasaka T, Togitani K, Koeffler HP, Yokoyama A: A novel treatment strategy targeting polo-like kinase 1 in hematological malignancies. Leukemia 2009;23:1564-1576.
63 Bucur O, Stancu AL, Goganau I, Petrescu SM, Pennarun B, Bertomeu T, Dewar R, Khosravi-Far R: Combination of bortezomib and mitotic inhibitors down-modulate Bcr-Abl and efficiently eliminates tyrosine-kinase inhibitor sensitive and resistant Bcr-Abl-positive leukemic cells. PLoS One 2013;8:e77390.

64 Hugle M, Belz K, Fulda S: Identification of synthetic lethality of PLK1 inhibition and microtubule-destabilizing drugs. Cell Death Differ 2015;22:1946-1956.
65 Czaplinski S, Hugle M, Stiehl V, Fulda S: Polo-like kinase 1 inhibition sensitizes neuroblastoma cells for vinca alkaloid-induced apoptosis. Oncotarget 2016;7:8700-8711.
66 Weiss LM, Hugle M, Romero S, Fulda S: Synergistic induction of apoptosis by a polo-like kinase 1 inhibitor and microtubule-interfering drugs in Ewing sarcoma cells. Int J Cancer 2016;138:497-506.
67 Abbou S, Lanvers-Kaminsky C, Daudigeos-Dubus E, LE Dret L, Laplace-Builhe C, Molenaar J, Vassal G, Geoerger B, within the IB, Preclinical Evaluation C: Polo-like Kinase Inhibitor Volasertib Exhibits Antitumor Activity and Synergy with Vincristine in Pediatric Malignancies. Anticancer Res 2016;36:599-609.
68 Van den Bossche J, Lardon F, Deschoolmeester V, De Pauw I, Vermorken JB, Specenier P, Pauwels P, Peeters M, Wouters A: Spotlight on Volasertib: Preclinical and Clinical Evaluation of a Promising Plk1 Inhibitor. Med Res Rev 2016;36:749-786.
69 Garcia-Manero G, Fenaux P, Al-Kali A, Baer MR, Sekeres MA, Roboz GJ, Gaidano G, Scott BL, Greenberg P, Platzbecker U, Steensma DP, Kambhampati S, Kreuzer KA; Godley LA, Atallah E, Collins R Jr, Kantarjian H, Jabbour E, Wilhelm FE, Azarnia N, et al.: Rigosertib versus best supportive care for patients with high-risk myelodysplastic syndromes after failure of hypomethylating drugs (ONTIME): a randomised, controlled, phase 3 trial. Lancet Oncol 2016;17:496-508.
70 Yim H: Current clinical trials with polo-like kinase 1 inhibitors in solid tumors. Anticancer Drugs 2013;24:999-1006.
71 El Dika I, Lim HY, Yong WP, Lin CC, Yoon JH, Modiano M, Freilich B, Choi HJ, CHao TY, Kelley RK, Brown J, Knox J, Ryoo BY, Yau T, Abou-Alfa GK:: An Open-Label, Multicenter, Phase I, Dose Escalation Study with Phase II Expansion Cohort to Determine the Safety, Pharmacokinetics, and Preliminary Antitumor Activity of Intravenous TKM-080301 in Subjects with Advanced Hepatocellular Carcinoma. Oncologist 2019;24:747-e218.
72 Olmos D, Barker D, Sharma R, Brunetto AT, Yap TA, Taegtmeyer AB, Barriuso J, Medani H, Degenhardt YY, Allred AJ, Smith DA, Murray SC, Lampkin TA, Dar MM, Wilson R, de Bono JS, Blagden SP: Phase I study of GSK461364, a specific and competitive Polo-like kinase 1 inhibitor, in patients with advanced solid malignancies. Clin Cancer Res 2011;17:3420-3430.
73 Weiss GJ, Jameson G, Von Hoff DD, Valsasina B, Davite C, Di Giulio C, Fiorentini F, Alzani R, Carpinelli P, Di Sanzo A, Galvani A, Isacchi A, Ramanathan RK: Phase I dose escalation study of NMS-1286937, an orally available Polo-Like Kinase 1 inhibitor, in patients with advanced or metastatic solid tumors. Invest New Drugs 2018;36:85-95.
74 Hikichi Y, Honda K, Hikami K, Miyashita H, Kaieda I, Murai S, Uchiyama N, Hasegawa M, Kawamoto T, Sato T, Ichikawa T, Cao S, Nie Z, Zhang L, Yang J, Kuida K, Kupperman E: TAK-960, a novel, orally available, selective inhibitor of polo-like kinase 1, shows broad-spectrum preclinical antitumor activity in multiple dosing regimens. Mol Cancer Ther 2012;11:700-709.
75 Garland LL, Taylor C, Pilkington DL, Cohen JL, Von Hoff DD: A phase I pharmacokinetic study of HMN-214, a novel oral stilbene derivative with polo-like kinase-1-interacting properties, in patients with advanced solid tumors. Clin Cancer Res 2006;12:5182-5189.
76 Moureau S, MacKay C, Saladino C, Pohler E, Kroboth K, Hollick J, Zheleva D, Frame S, Blake D: The novel PLK1 inhibitor, CYC140: Identification of pharmacodynamic markers, sensitive target indications and potential combinations [abstract]. Cancer Res 2017;77:Abstract nr 4178.